

# Joint Turbo Equalization and Carrier Synchronization for SC-FDE Schemes

Rui Dinis<sup>(1,2)</sup>, Teresa Araújo<sup>(1,3)</sup>, Pedro Pedrosa<sup>(1,4)</sup> and Fernando Nunes<sup>(1,4)</sup>

<sup>(1)</sup>Instituto de Telecomunicações, Lisbon, Portugal

<sup>(2)</sup>FCT-UNL, Monte da Caparica, Portugal

<sup>(3)</sup>ISEP, Porto, Portugal

<sup>(4)</sup>IST, Lisbon, Portugal

## ABSTRACT

In this paper we consider the use of SC (Single-Carrier) modulations combined with FDE (Frequency-Domain Equalization) in future broadband wireless systems. We propose iterative receiver structures with joint equalization and carrier synchronization. The proposed receivers can be regarded as modified frequency-domain turbo equalizers where we perform a decision-directed frequency offset estimation within each iteration of the turbo equalizer.

Our performance results show that the proposed receiver structure has good BER (Bit Error Rate), even with moderate frequency offsets and in severely time-dispersive channels. Moreover, our receiver has a relatively low implementation complexity, due to its FFT-based (Fast Fourier Transform) frequency-domain implementation.<sup>1</sup>

**Keywords:** Frequency-domain equalization, turbo equalization, carrier synchronization, iterative receivers

## I. INTRODUCTION

Due to an increased demand for wireless services, future systems are required to support high quality of service at high data rates. For such high data rates, the time-dispersion effects associated to the multipath propagation can be severe. In this case, conventional time-domain equalization schemes are not practical.

<sup>1</sup>This work was partially supported by the FCT the - Fundação para a Ciência e Tecnologia (pluriannual funding, U-BOAT project PTDC/EEA-TEL/67066/2006 and PhD grants SFRH/BD/29682/2006 and SFRH/BD/????). Part of this research was published in IEEE GLOBECOM'04.

Block transmission techniques, with appropriate cyclic extensions and employing FDE techniques (Frequency-Domain Equalization), have been shown to be suitable for high data rate transmission over severely time-dispersive channels without requiring complex receivers.

The most popular modulations based on this concept are the OFDM modulations (Orthogonal Frequency Division Multiplexing) [1]. Block transmission SC modulations (Single Carrier) combined with FDE (also denoted SC-FDE), are an alternative approach based on this principle [2]. Like OFDM modulations, the data blocks are preceded by a cyclic prefix, long enough to cope with the channel impulse response length. The received signal is transformed to frequency domain, equalized in frequency domain and then transformed back to time domain.

Although OFDM has very poor uncoded performance [3], the achievable performances with appropriate channel coding are similar for OFDM and SC/FDE [4], [5]. In terms of implementation complexity, OFDM schemes need an IDFT (Inverse Discrete Fourier Transform) operation at the transmitter and an DFT operation at the receiver; for SC-FDE, a pair DFT/IDFT is needed at the receiver (no DFT or IDFT is required at the transmitter). Therefore, the overall implementation complexities for SC-FDE and OFDM schemes are similar, although the OFDM receivers are slightly simpler and the transmitters more complex. Moreover, the OFDM signals have larger envelope fluctuations which lead to amplification difficulties. Therefore, the OFDM schemes are clearly preferable for the downlink (i.e., the transmission from the BS (Base Station) to the MT (Mobile Terminal)) and the SC-FDE schemes are preferable for the uplink (i.e., the transmission from the MT to the BS). For this reason, a mixed SC/OFDM air interface was proposed [4], [6], with an OFDM scheme in the downlink and a SC-FDE scheme in the uplink. In this paper we consider only the uplink transmission of this type of system, i.e., an SC-FDE approach.

A promising IFDE (Iterative FDE) technique for SC-FDE, denoted IB-DFE (Iterative Block-Decision Feedback Equalizer), was proposed in [7]. This technique was later extended to diversity scenarios [5] and layered space-time schemes [8]. These IFDE receivers can be regarded as iterative DFE receivers with the feedforward and the feedback operations implemented in the frequency domain. Since the feedback loop takes into account not just the hard-decisions for each block but also the overall block reliability, we have small error propagation. Consequently, IFDE techniques offer much better performances than the non-iterative methods [5], [7], [8]. Within these IFDE receivers the equalization and channel decoding procedures are performed separately (i.e., the feedback loop uses the equalizer outputs instead of the channel decoder outputs). However, it is known that higher performance gains can be achieved if these procedures are performed jointly. An effective way of achieving this is by employing the so-called turbo equalization schemes where the equalization and decoding procedures are repeated, in an iterative way,

with some soft information being passed between them [9]. Although initially proposed for time-domain receivers, turbo equalizers also allow frequency-domain implementations [10], [11]<sup>2</sup>.

In order to maintain high power and spectral efficiencies, the cyclic prefix, which is longer than the overall channel impulse response length, should be a small fraction of the block duration. Therefore, we usually need large blocks for severely time-dispersive channels, with hundreds or even thousands of symbols. Typically, the frequency errors cannot exceed a small fraction of the inverse of the block duration. This means that we have higher sensitivity to frequency errors for larger blocks, making accurate carrier synchronization mandatory. One source of frequency errors is the frequency mismatch between the oscillators at the transmitter and receiver. Another possible source of frequency errors is the Doppler frequency shift caused by relative motion between the transmitter and the receiver.

The carrier synchronization is usually performed in two (or more) stages. Typically a coarse synchronization, with moderate accuracy and large acquisition band, is followed by a fine synchronization, with high accuracy and small acquisition band ([12], and references therein). The fine carrier synchronization can be performed after the equalization procedure. This is especially effective for SC modulations since the frequency offsets produce a progressive constellation rotation and the equalized signal resembles the received signal in flat-fading channels [13].

Alternatively to consider a decision-directed CFO (Carrier Frequency Offset) estimator, estimates may be obtained using known sequences with good correlation properties. Although yielding more accurate estimates, this solution requires an extra block overhead thus reducing the bandwidth efficiency [14]. Exploring the similarities between the synchronization requirements of both transmission schemes, it is possible to use, in SC-FDE schemes, the frame structure of training symbols originally designed for synchronization purposes in OFDM schemes. In [15], Moose proposed a Maximum-Likelihood (ML) CFO estimator, based on the use of two identical and consecutive symbols, with a frequency acquisition range  $\pm 1/(2T)$ , where  $T$  is the "useful" symbol duration. This result was later extended in [16], which uses also two symbols; the first estimates the fractional part of the CFO ( $|\Delta f| < 1/T$ ), whereas the second symbol resolves the frequency ambiguity inherent in the first symbol, i.e., it estimates the integer part of the CFO ( $\Delta f$  multiple of  $1/T$ ). Morelli and Mengali proposed in [17] an algorithm exploiting a training symbol with  $L > 2$  identical parts. Its estimation range is  $\pm L/2$  times the subcarrier spacing and its accuracy is slightly superior to that of the Schmidl and Cox method. Its main advantage is that it

<sup>2</sup>The IFDEs of [5], [7], [8] (or IB-DFEs) can be regarded as special types of frequency-domain turbo equalizers with reduced complexity, since the channel decoder is not required in the feedback loop.

needs just one training symbol while the Schmidl and Cox method needs two symbols. In [18], Morelli and Mengali improved this estimation technique using algorithms that achieve the Cramer-Rao bound at the cost of increased complexity. A comparison between different designs for the frame structure of the pilot symbols is made in [19]. Besides pilot tone-aided algorithms, other techniques, like cyclic-prefix estimation, may be applied to track the frequency offset (see, for instance, [20]).

In this paper we consider an SC-FDE block transmission in the presence of residual frequency errors. We propose a receiver structure with joint equalization and carrier synchronization. We consider iterative receivers that can be regarded as modified frequency-domain turbo equalizers where we perform decision-directed frequency offset estimation within each iteration of the turbo equalizer.

This paper is organized as follows. The basic iterative FDE receivers are described in sec. II. Sec. III presents the modified receivers with joint equalization and carrier synchronization. A set of performance results is presented in sec. IV and sec. V is concerned with the conclusions.

## II. ITERATIVE FDE RECEIVERS

### A. Receiver Structure

For the sake of simplicity, we will assume in this section that there is perfect carrier synchronization. Fig. 1(A) presents the iterative frequency-domain receiver structure considered in this paper. It is assumed that we have  $L$  receiver antennas, i.e., we have  $L$ -order space diversity. The received time-domain block associated to the  $l$ th antenna,  $\{y_n^{(l)}; n = 0, 1, \dots, N - 1\}$ , is passed to the frequency domain by a DFT operation, leading to the block  $\{Y_k^{(l)}; k = 0, 1, \dots, N - 1\}$ , with

$$Y_k^{(l)} = S_k H_k^{(l)} + N_k^{(l)}, \quad (1)$$

where  $H_k^{(l)}$  and  $N_k^{(l)}$  denote the channel transfer function and the channel noise, respectively, for the  $k$ th subchannel of the  $l$ th diversity branch. The block of frequency-domain symbols  $\{S_k; k = 0, 1, \dots, N - 1\}$  is the DFT of the transmitted time-domain block,  $\{s_n; n = 0, 1, \dots, N - 1\}$ , with  $s_n$  denoting the  $n$ th data symbol to be transmitted, selected from a given constellation (e.g., a QAM or a PSK constellation).

For a given iteration  $i$ , the frequency-domain samples at the output of the FDE are given by<sup>3</sup>

$$\tilde{S}_k^{(i)} = \sum_{l=1}^L F_k^{(l,i)} Y_k^{(l)} - B_k^{(i)} \overline{S}_k^{(i-1)} \quad (2)$$

<sup>3</sup>Our IFDE receiver is slightly different from the IB-DFE receivers of [5] and [7], since there the correlation factor is incorporated in the feedback coefficients.

where  $\{F_k^{(l,i)}; k = 0, 1, \dots, N-1\}$  ( $l = 1, 2, \dots, L$ ) are the feedforward coefficients and  $\{B_k^{(i)}; k = 0, 1, \dots, N-1\}$  are the feedback coefficients.  $\{\bar{S}_k^{(i-1)}; k = 0, 1, \dots, N-1\}$  denotes the DFT of the block of time-domain average symbol values associated to the previous iteration,  $\{\bar{s}_n^{(i-1)}; n = 0, 1, \dots, N-1\}$ . The method for obtaining these average values is described in subsection II-B.

It can be shown that the optimum feedback coefficients are [5], [7]<sup>4</sup>

$$B_k^{(i)} = \sum_{l=1}^L F_k^{(l,i)} H_k^{(l)} - 1 \quad (3)$$

and the feedforward coefficients are given by

$$F_k^{(l,i)} = \frac{\check{F}_k^{(l,i)}}{\gamma^{(i)}}, \quad (4)$$

with

$$\check{F}_k^{(l,i)} = \frac{H_k^{(l)*}}{\alpha + (1 - (\rho^{(i-1)})^2) \sum_{l=1}^L |H_k^{(l)}|^2}, \quad (5)$$

where  $\alpha = E[|N_k^{(l)}|^2]/E[|S_k|^2]$ . In (4) we have

$$\gamma^{(i)} = \frac{1}{N} \sum_{k=0}^{N-1} \sum_{l=1}^L \check{F}_k^{(l,i)} H_k^{(l)} \quad (6)$$

and the correlation factor  $\rho^{(i-1)}$  in (5) is defined as

$$\rho^{(i-1)} = \frac{E[\hat{s}_n^{(i-1)} s_n^*]}{E[|s_n|^2]}, \quad (7)$$

where the block  $\{\hat{s}_n^{(i-1)}; n = 0, 1, \dots, N-1\}$  denotes the data estimates associated to the previous iteration, i.e., the hard-decisions associated to the time-domain block at the output of the FDE,  $\{\bar{s}_n^{(i)}; n = 0, 1, \dots, N-1\} = \text{IDFT} \{\tilde{S}_k^{(i)}; k = 0, 1, \dots, N-1\}$ .

It should be noted that

$$F_k^{(l,i)} = H_k^{(l)*} C_k^{(i)}, \quad (8)$$

with

$$C_k^{(i)} = \frac{1/\gamma^{(i)}}{\alpha + (1 - (\rho^{(i-1)})^2) \sum_{l=1}^L |H_k^{(l)}|^2}. \quad (9)$$

Therefore, the receiver structure of fig. 1(A) is equivalent to the receiver structure of fig. 1(B), where only  $C_k^{(i)}$  changes with the iteration order.

<sup>4</sup>Contrarily to [5] and [7], we are considering normalized equalizers, i.e.,  $\frac{1}{N} \sum_{k=0}^{N-1} \sum_{l=1}^L F_k^{(l,i)} H_k^{(l)} = 1$ .

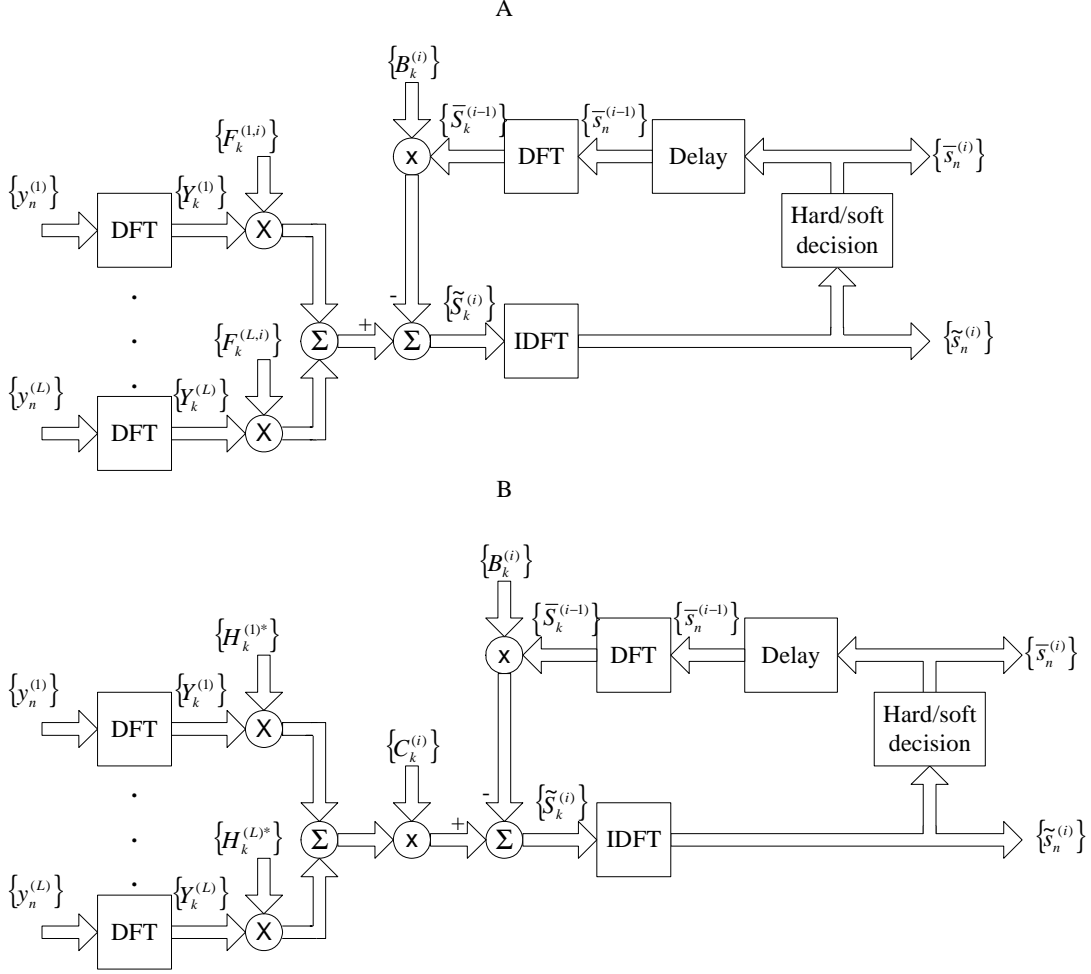


Fig. 1. (A) IFDE receiver with  $L$ -branch space diversity and (B) equivalent receiver structure, since  $F_k^{(l,i)} = H_k^{(l)*} C_k^{(i)}$ ,  $l = 1, 2, \dots, L$ .

### B. Computation of the Average Values and the Correlation Factor

Clearly,  $\rho^{(i)}$  can be regarded as the blockwise reliability of the estimates  $\{\hat{s}_n^{(i)}; n = 0, 1, \dots, N - 1\}$ . This means that we can define the "blockwise average" symbols as  $\{\bar{s}_n^{(i)} = \rho^{(i)} \hat{s}_n^{(i)}; n = 0, 1, \dots, N - 1\}$ .

In order to improve the performance of the receiver, we may replace the "blockwise averages" by "symbol averages". In addition, this provides an expedite way of computing the blockwise reliabilities.

Assume that the transmitted symbols are selected from a QPSK constellation under a Gray mapping rule (the generalization to other cases is straightforward). We define  $s_n = \pm 1 \pm j = s_n^I + j s_n^Q$ , with  $s_n^I = \text{Re}\{s_n\} = \pm 1$  and  $s_n^Q = \text{Im}\{s_n\} = \pm 1$ ,  $n = 0, 1, \dots, N - 1$  (similar definitions can be made for

$\tilde{s}_n = \tilde{s}_n^I + j\tilde{s}_n^Q$ ,  $\hat{s}_n = \hat{s}_n^I + j\hat{s}_n^Q$  and  $\bar{s}_n = \bar{s}_n^I + j\bar{s}_n^Q$ ).

The LLRs (LogLikelihood Ratios) of the "in-phase bit" and the "quadrature bit", associated to  $s_n^{I(i)}$  and  $s_n^{Q(i)}$ , respectively, are given by<sup>5</sup>

$$L_n^{I(i)} = \frac{2}{\sigma_i^2} \tilde{s}_n^{I(i)} \quad (10)$$

and

$$L_n^{Q(i)} = \frac{2}{\sigma_i^2} \tilde{s}_n^{Q(i)}, \quad (11)$$

respectively, where

$$\sigma_i^2 = \frac{1}{2} E[|s_n - \tilde{s}_n^{(i)}|^2] \approx \frac{1}{2N} \sum_{n=0}^{N-1} E[|\hat{s}_n^{(i)} - \tilde{s}_n^{(i)}|^2]. \quad (12)$$

Under a Gaussian assumption, it can be shown that the mean value of  $s_n$  is

$$\bar{s}_n^{(i)} = \tanh\left(\frac{L_n^{I(i)}}{2}\right) + j \tanh\left(\frac{L_n^{Q(i)}}{2}\right). \quad (13)$$

Clearly, the hard decisions  $\hat{s}_n^{I(i)} = \pm 1$  and  $\hat{s}_n^{Q(i)} = \pm 1$  are defined according to the signs of  $L_n^{I(i)}$  and  $L_n^{Q(i)}$ , respectively. Therefore,  $\bar{s}_n^{(i)} = \rho_n^{I(i)} \hat{s}_n^{I(i)} + j \rho_n^{Q(i)} \hat{s}_n^{Q(i)}$ , where

$$\begin{aligned} \rho_n^{I(i)} &= \frac{E[s_n^I \hat{s}_n^{I(i)}]}{E[|s_n^I|^2]} = \\ &= 1 - 2 \text{Prob}(\hat{s}_n^{I(i)} \neq s_n^I) = \tanh\left(\frac{|L_n^{I(i)}|}{2}\right) \end{aligned} \quad (14)$$

and

$$\begin{aligned} \rho_n^{Q(i)} &= \frac{E[s_n^Q \hat{s}_n^{Q(i)}]}{E[|s_n^Q|^2]} = \\ &= 1 - 2 \text{Prob}(\hat{s}_n^{Q(i)} \neq s_n^Q) = \tanh\left(\frac{|L_n^{Q(i)}|}{2}\right). \end{aligned} \quad (15)$$

Quantities  $\rho_n^{I(i)}$  and  $\rho_n^{Q(i)}$  can be regarded as the reliabilities associated to the "in-phase" and "quadrature" bits of the  $n$ th symbol (naturally,  $0 \leq \rho_n^{I(i)} \leq 1$  and  $0 \leq \rho_n^{Q(i)} \leq 1$ ). For the first iteration,  $\rho_n^{I(i)} = \rho_n^{Q(i)} = 0$  and  $\bar{s}_n^{(i)} = 0$ ; after some iterations and/or when the SNR (Signal-to-Noise Ratio) is high, typically  $\rho_n^{I(i)} \approx 1$  and  $\rho_n^{Q(i)} \approx 1$ , leading to  $\bar{s}_n \approx \hat{s}_n^{(i)}$ . The feedforward coefficients are still obtained from (4)-(5), but with the blockwise reliability given by

$$\rho^{(i)} = \frac{1}{N} \sum_{n=0}^{N-1} \frac{E[s_n^* \hat{s}_n^{(i)}]}{E[|s_n|^2]} = \frac{1}{2N} \sum_{n=0}^{N-1} (\rho_n^{I(i)} + \rho_n^{Q(i)}). \quad (16)$$

<sup>5</sup>Once again, it is assumed that  $\gamma^{(i)} = 1$ , i.e., we have a normalized FDE.

The receiver with "blockwise reliabilities", denoted in the following as IFDE-HD (Iterative FDE with Hard Decisions), and the receiver with "symbol reliabilities", denoted in the following as IFDE-SD (IFDE with Soft Decisions), employ the same feedforward coefficients; however, in the former, the feedback loop uses the "hard-decisions" on each data block, weighted by a common reliability factor, while in the latter, the reliability factor changes from symbol to symbol (in fact, the reliability factor is different in the real and imaginary component of each symbol). The IB-DFE scheme considered in [5], [7] corresponds to the IFDE-HD, since "blockwise reliabilities" were considered there.

### C. Use of Channel Decoder Outputs in the Feedback Loop

We can define a frequency-domain turbo equalizer that employs the channel decoder outputs instead of the uncoded "soft decisions" in the feedback loop. The receiver structure, that will be denoted Turbo FDE, is similar to the IFDE-SD, but with a SISO (Soft-In, Soft-Out) channel decoder employed in the feedback loop. The SISO block, that can be implemented as defined in [21], provides the LLRs of both the "information bits" and the "coded bits". The input of the SISO block are LLRs of the "coded bits" at the FDE output, given by (10) and (11). Once again, the feedforward coefficients are obtained from (4)-(5), with the blockwise reliability given by (16).

## III. JOINT EQUALIZATION AND CARRIER SYNCHRONIZATION

### A. Receiver Structure

Let us assume now that there is a residual frequency offset  $\Delta f$  between the transmitter and the receiver local oscillators. In this case, the received time-domain block associated to the  $l$ th diversity branch is  $\{y_n^{(l)}; n = 0, 1, \dots, N - 1\}$  and the corresponding frequency-domain blocks are  $\{Y_k^{(l)}; k = 0, 1, \dots, N - 1\}$ , with

$$Y_k^{(l)} = S'_k H_k^{(l)} + N_k^{(l)}, \quad (17)$$

where the block of frequency-domain symbols  $\{S'_k; k = 0, 1, \dots, N - 1\}$  is the DFT of the effectively transmitted block of time-domain data symbols,  $\{s'_n; n = 0, 1, \dots, N - 1\}$ , with

$$s'_n = s_n \exp\left(j2\pi \frac{\Delta f n T}{N}\right). \quad (18)$$

For the sake of simplicity, it is assumed that the residual frequency offset results exclusively from the transmitter (i.e., the MT, since we are considering the uplink); we also assume that the phase rotation is 0 for  $n = 0$ .

Clearly, the residual frequency offset leads to a progressive phase rotation of the time-domain symbols at the FDE output. Since this phase rotation might lead to significant performance degradation, we will modify our receiver so as to estimate and compensate the phase rotation associated to the frequency offset. Fig. 2 presents a receiver with joint equalization and frequency offset estimation and compensation. This receiver is based on the basic FDE described in fig. 1(A) (the extension to the receiver format of fig. 1(B) is straightforward), and the receiver parameters are obtained in a similar way. However, for each iteration we perform the frequency offset estimation and compensation before the detection procedure. Once again, we can have either hard decisions or soft decisions (IFDE-HD or IFDE-SD, respectively); we can also use the channel decoder outputs in the feedback loop (Turbo FDE). For each iteration, the frequency offset is estimated as described in the following subsection.

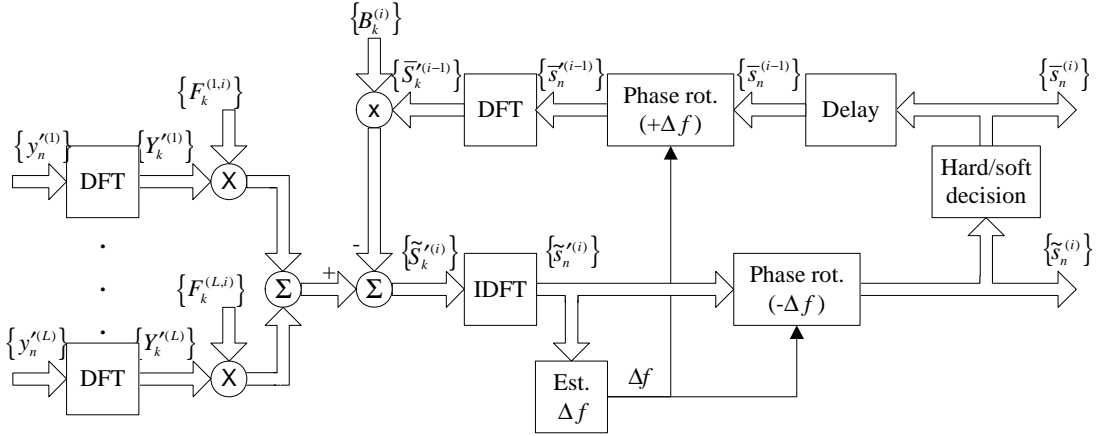


Fig. 2. Proposed receiver for joint equalization and carrier synchronization.

### B. Frequency Offset Estimation

Let us assume a slowly-varying scenario. In this case, the overall channel at the output of the FDE can be regarded as a stationary flat fading channel (at least for the duration of a given block). Therefore, we can describe the frequency offset estimation procedure assuming an ideal Gaussian channel.

In the presence of a frequency offset  $\Delta f$ , the received block is  $\{y'_n = s'_n + \nu_n; n = 0, 1, \dots, N - 1\}$ , where  $s'_n$  is given by (18) and  $\nu_n$  is the Gaussian noise component, with  $E[\nu_n] = 0$  and  $E[|\nu_n|^2] = 2\sigma^2$  ( $\sigma^2$  denotes the variance of both real and imaginary parts of  $\nu_n$ ).

If the transmitted symbols are known we can estimate the frequency offset in the following way:

$$\widehat{\Delta f} = \frac{N}{2\pi MT} \arg \{ \xi \}, \quad (19)$$

with

$$\xi = \sum_{n=0}^{N-M-1} y'_{n+M} y_n'^* s_{n+M}^* s_n = \bar{\xi} + \varepsilon, \quad (20)$$

for an appropriate  $M$ , where  $\bar{\xi} = E[\xi]$  and  $\varepsilon$  is an error term. Clearly,  $s_{n+M}^* s_n$  is used to wipe out the phase modulation in  $y'_{n+M} y_n'^*$ . For the sake of simplicity, we are assuming  $|s_n| = s$ , i.e., we are employing constant amplitude constellations (e.g., a PSK constellation), thus yielding

$$y'_{n+M} y_n'^* s_{n+M}^* s_n = s^4 \exp \left( j2\pi \frac{\Delta f MT}{N} \right) + \varepsilon_n, \quad (21)$$

where the channel noise contribution is allotted to  $\varepsilon_n$ ; since  $E[\varepsilon_n] = 0$ ,

$$\bar{\xi} = E[|s_n|^2]^2 (N - M) \exp \left( j2\pi \frac{\Delta f MT}{N} \right). \quad (22)$$

It can be shown that, for high SNR, the frequency offset estimate given by (19) is unbiased, with variance

$$\sigma_{\Delta f}^2 = E[|\widehat{\Delta f} - \Delta f|^2] = \left( \frac{N}{2\pi MT} \right)^2 \frac{\sigma_{\varepsilon_Q}^2}{|\bar{\xi}|^2}, \quad (23)$$

with  $\sigma_{\varepsilon_Q}^2$  denoting the variance of the quadrature component of  $\varepsilon_n$  (for  $\Delta f = 0$  this corresponds to the variance of the imaginary part of the noise). It is shown in Appendix A that, for high SNR, this variance is approximately given by

$$\sigma_{\varepsilon_Q}^2 \approx \begin{cases} s^8(N - M)/\text{SNR}, & M > N/2 \\ s^8 M/\text{SNR}, & M < N/2, \end{cases} \quad (24)$$

with

$$\text{SNR} = \frac{E[|s_n|^2]}{E[|\nu_n|^2]}. \quad (25)$$

This means that

$$\sigma_{\Delta f}^2 \approx \frac{1}{\text{SNR}(2\pi T)^2} \frac{N^2}{M^2(N - M)} \quad (26)$$

for  $M > N/2$  and

$$\sigma_{\Delta f}^2 \approx \frac{1}{\text{SNR}(2\pi T)^2} \frac{N^2}{M(N - M)^2} \quad (27)$$

for  $M < N/2$  (thus,  $\sigma_{\Delta f}^2$  takes the same values for  $M = M_0$  and  $M = N - M_0$ ).

It can easily be shown that there are two optimum values for  $M$ ,  $M = 2N/3$  and  $M = N/3$ , both corresponding to

$$\sigma_{\Delta f}^2 \approx \frac{1}{\text{SNR}(2\pi T)^2} \frac{27}{4N}. \quad (28)$$

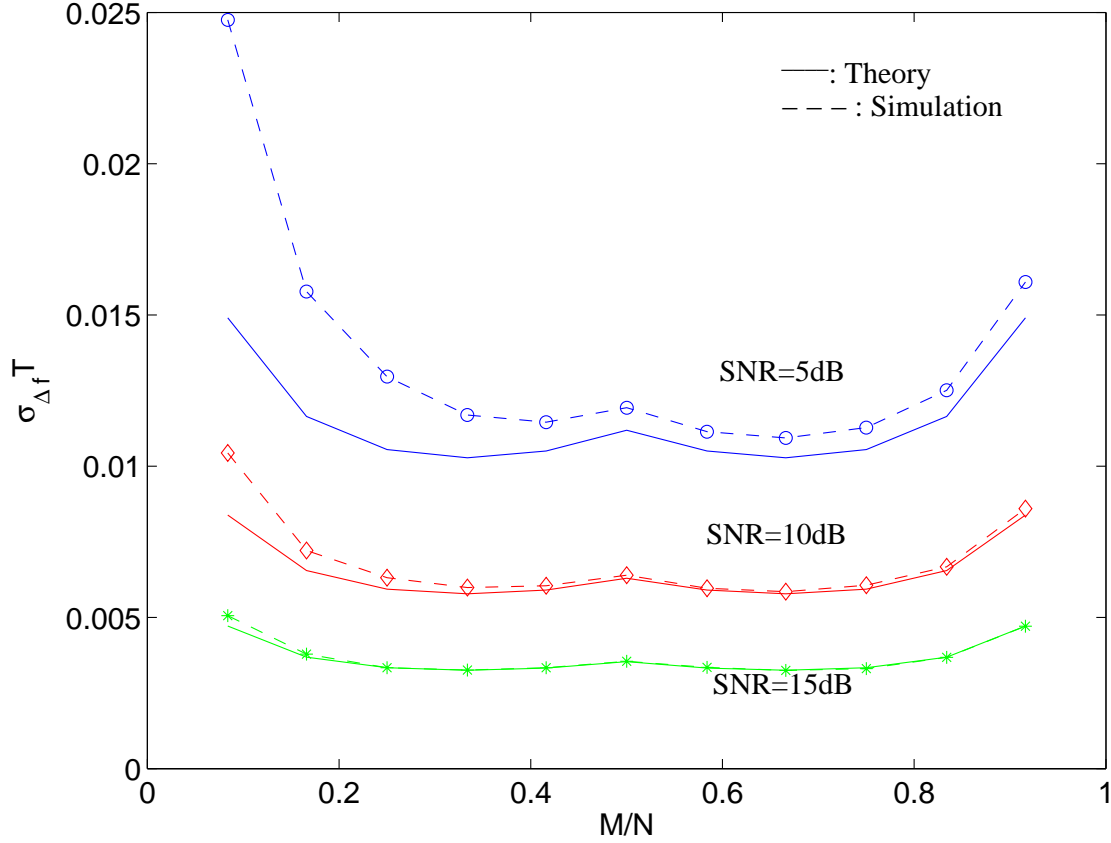


Fig. 3. Impact of  $M/N$  on  $\sigma_{\Delta f}T$ .

Fig. 3 shows the impact of  $M/N$  on  $\sigma_{\Delta f}T$  when  $N = 512$ . Clearly, we have almost the same performance for a wide range of values of  $M/N$ , provided that  $M$  is not too close to  $N$  nor too small. For moderate-to-high SNR values, the theoretical values of  $\sigma_{\Delta f}T$ , given by (28), are close to the simulated ones; for low SNR the theoretical values are slightly better than the simulated ones (the differences are higher for  $M < N/2$ , especially for smaller values of  $M$ ). Moreover, the optimum value of  $M$  is independent of the actual SNR.

Since the  $n$ th data symbol is rotated by  $n\theta$ , with  $\theta = 2\pi\Delta fT/N$ , the corresponding BER for a QPSK

constellation and an ideal Gaussian channel is<sup>6</sup>

$$P_{b,n} = \frac{1}{2}Q \left( \sqrt{2\frac{E_b}{N_0}}(\cos(n\theta) - \sin(n\theta)) \right) + \frac{1}{2}Q \left( \sqrt{2\frac{E_b}{N_0}}(\cos(n\theta) + \sin(n\theta)) \right). \quad (29)$$

( $2E_b/N_0 = \text{SNR}$ ) and the overall BER is the average of  $P_{b,n}$  over  $n$ . Fig. 4 shows the impact of the frequency offset on the BER. Clearly, we can have an almost ideal performance if  $\Delta fT \leq 0.025$ ; with  $\Delta fT = 0.05$  we have about 2dB of degradation at  $\text{BER}=10^{-4}$ . This means that the accuracy of the proposed frequency offset estimation method is more than enough for typical SNR and moderate-to-long blocks.

Naturally, the frequency-offset estimation method described above requires the knowledge of the transmitted symbols  $s_n$ . Since they are not known at the receiver, we can replace the symbol estimates by their average values from the previous iteration, i.e., for the  $i$ th iteration (20) takes the form

$$\xi = \sum_{n=0}^{N-M-1} y'_{n+M} y_n^* \bar{s}_{n+M}^{(i-1)*} \bar{s}_n^{(i-1)}. \quad (30)$$

#### IV. PERFORMANCE RESULTS

In this section we present a set of performance results concerning the joint equalization and carrier synchronization technique proposed in this paper. We consider SC-FDE modulations with blocks of  $N = 512$  "useful" modulation symbols (corresponding to a duration of  $4\mu\text{s}$ ), plus an appropriate cyclic prefix. The modulation symbols belong to a QPSK constellation and are selected from the transmitted data according to a Gray mapping rule. The channel encoder is the well-known rate-1/2 64-state convolutional code<sup>7</sup> with generators  $1 + D^2 + D^3 + D^5 + D^6$  and  $1 + D + D^2 + D^3 + D^6$ . Additionally, the coded bits are interleaved before being mapped into the constellation points. We consider linear power amplification and perfect channel estimation. The propagation channel is characterized by the power delay profile type C for HIPERLAN/2 (High PERFORMANCE Local Area Network) [22], with uncorrelated Rayleigh fading on the different paths (similar results could be obtained for other severely time-dispersive channel models with rich multipath propagation). The channels associated to different diversity branches are uncorrelated.

Let us first consider the performance of the different iterative FDE receivers under perfect carrier synchronization. Fig. 5 shows uncoded BER performances for IFDE-HD and IFDE-SD, without diversity

<sup>6</sup>Naturally, this means that there is no compensation of the frequency offset.

<sup>7</sup>It should be pointed out that more powerful coding schemes, such as the well-known turbo codes, could be employed. We selected a convolutional code due to its good performance with small blocks, not requiring interblock interleaving.

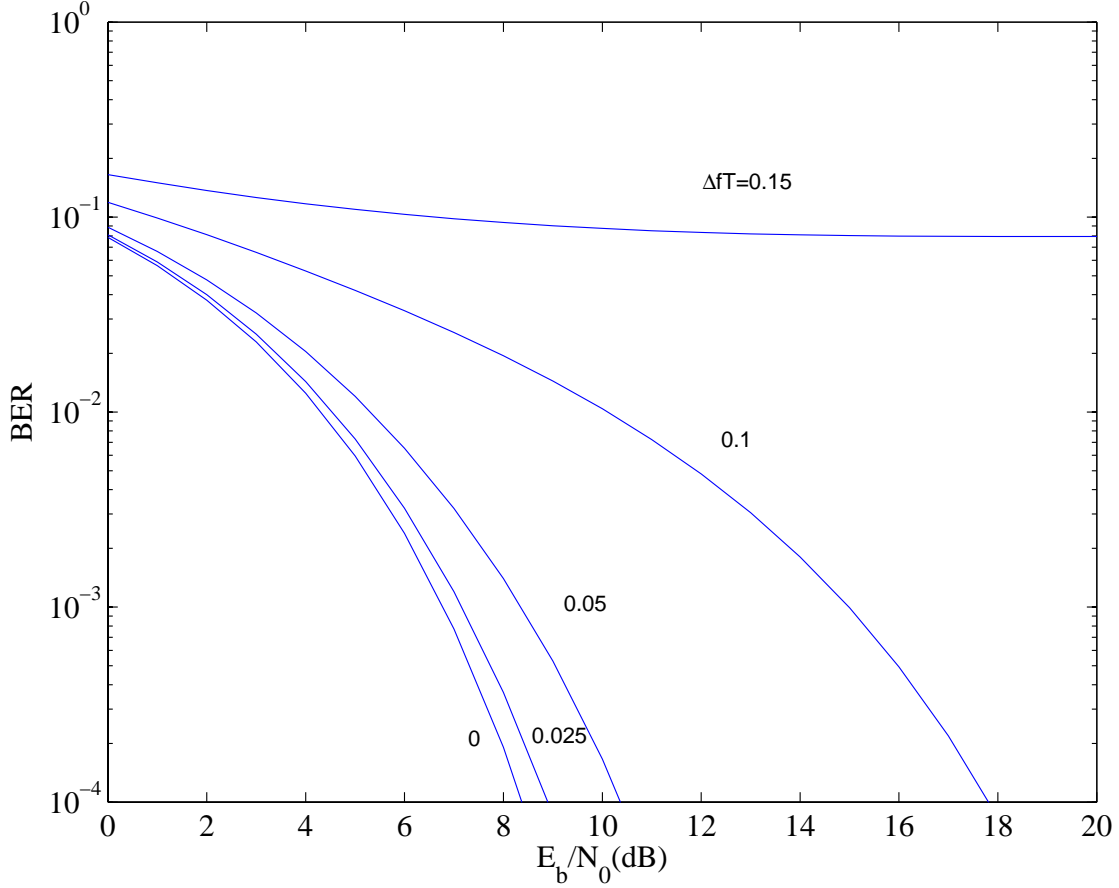


Fig. 4. BER for QPSK with several normalized frequency offsets  $\Delta fT$ .

( $L = 1$ ) and with two-branch space diversity ( $L = 2$ ). We also include the MFB (Matched Filter Bound) performance, defined as [5]

$$P_{b,MFB} = E \left[ Q \left( \sqrt{\frac{2E_b}{N_0} \frac{1}{N} \sum_{k=0}^{N-1} \sum_{l=1}^L |H_k^{(l)}|^2} \right) \right]. \quad (31)$$

From this figure, we can observe that there is a significant gain associated to the iterative procedure, especially without diversity ( $L = 1$ ). Moreover, the asymptotic performances can be very close to the MFB after just a few iterations. Notice that the performances with hard decisions (IFDE-HD) and soft decisions (IFDE-SD) are very similar, especially with diversity ( $L = 2$ ). Fig. 6 shows the coded BER performances for IFDE-SD and Turbo FDE. Clearly, the performance of the Turbo FDE is better, with gains above 1dB.

Let us consider now the impact of frequency offsets. For the sake of simplicity, it is assumed that the

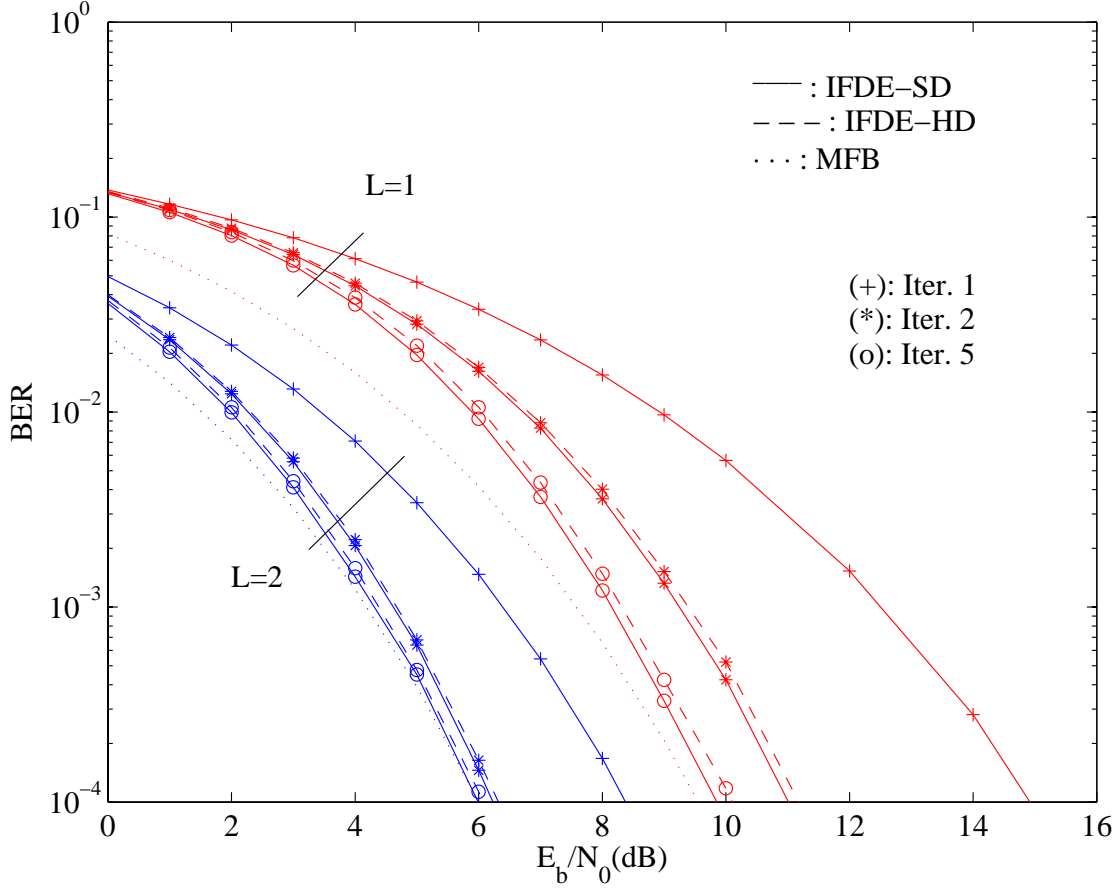


Fig. 5. Uncoded BER performance for IFDE-HD and IFDE-SD, together with the MFB.

linear phase rotation associated to the frequency offset starts from zero, as in (18).

Fig. 7 presents the evolution of  $E[\widehat{\Delta f} - \Delta f]$  for  $L = 1$  and an IFDE-SD, when  $\Delta f T = 0.05$  or  $0.1$  (similar performances were obtained for IFDE-HD; for  $L = 2$  we could obtain similar conclusions, since the curves are essentially shifted to the left). Clearly, the frequency offset estimates are biased, although the bias decreases with the number of iterations and with  $E_b/N_0$ . This bias is a consequence of the decision errors before estimating  $\Delta f$ . Figs. 8 and 9 present the corresponding uncoded BER performances. For the sake of comparison, we also include results without frequency offset estimation and with perfect frequency offset estimation. Clearly, the IFDE-SD has good asymptotic performances when  $\Delta f T = 0.05$ , approaching the performances with perfect frequency offset estimation after just a few iterations; for  $\Delta f T = 0.1$  we have a degradation of about 1dB relative to the case with perfect carrier synchronization. Regarding the coded BER, depicted in fig. 10, the difference relative to the case with

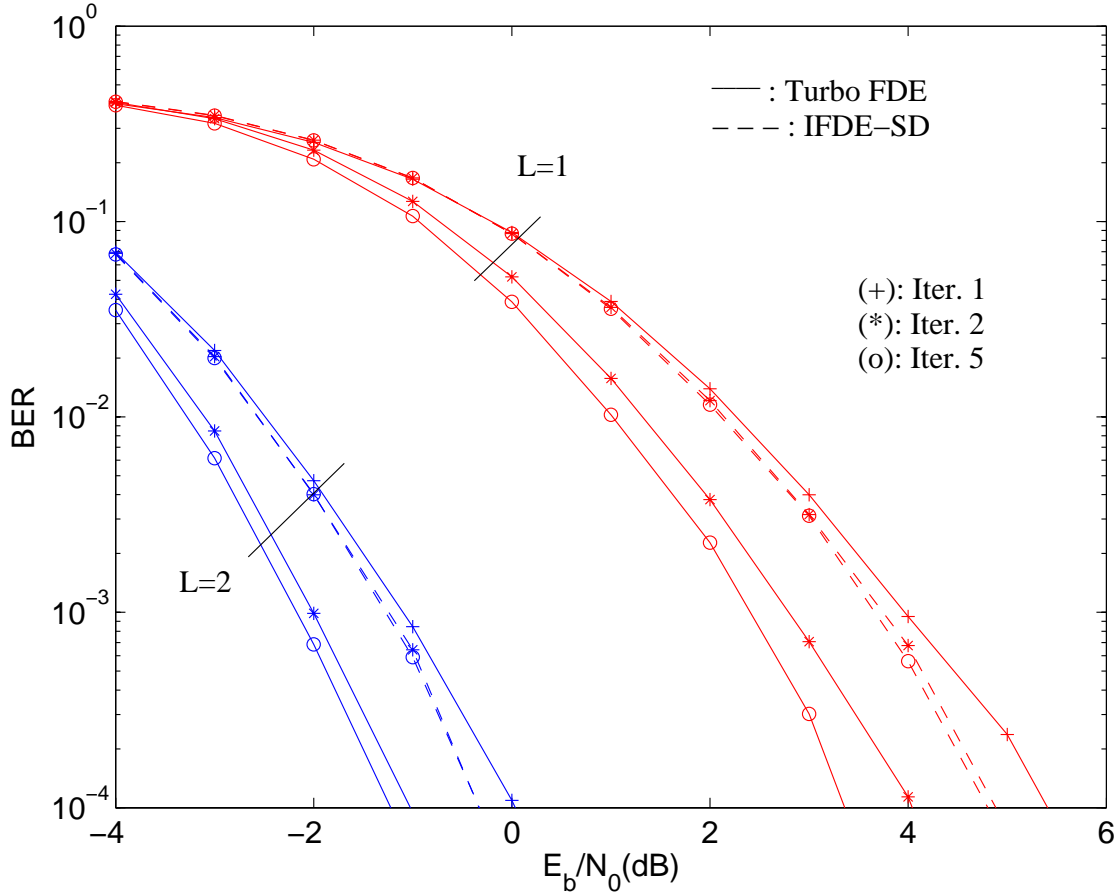


Fig. 6. Coded BER performance for IFDE-HD and IFDE-SD.

perfect carrier synchronization is less than 0.5dB and about 2dB for  $\Delta fT = 0.05$  and 0.1, respectively.

Let us consider now the Turbo FDE, with coded feedback using a SISO decoder, implemented through the Max-Log-MAP approach [21]. Fig. 11 presents the evolution of  $E[\widehat{\Delta f} - \Delta f]$  for a Turbo FDE with  $L = 1$ , when  $\Delta fT = 0.1$  or 0.15 (i.e., higher frequency offsets). Compared with the results of fig. 11, the bias of the frequency offset estimates are much lower at low SNR. The corresponding BER is depicted in fig. 12. Clearly, the Turbo FDE can cope with larger frequency offsets.

## V. CONCLUSIONS

In this paper we considered the use of SC-FDE with joint equalization and frequency offset estimation. We have an iterative receiver that estimates the residual frequency offset using estimates of the transmitted symbols for each iteration.

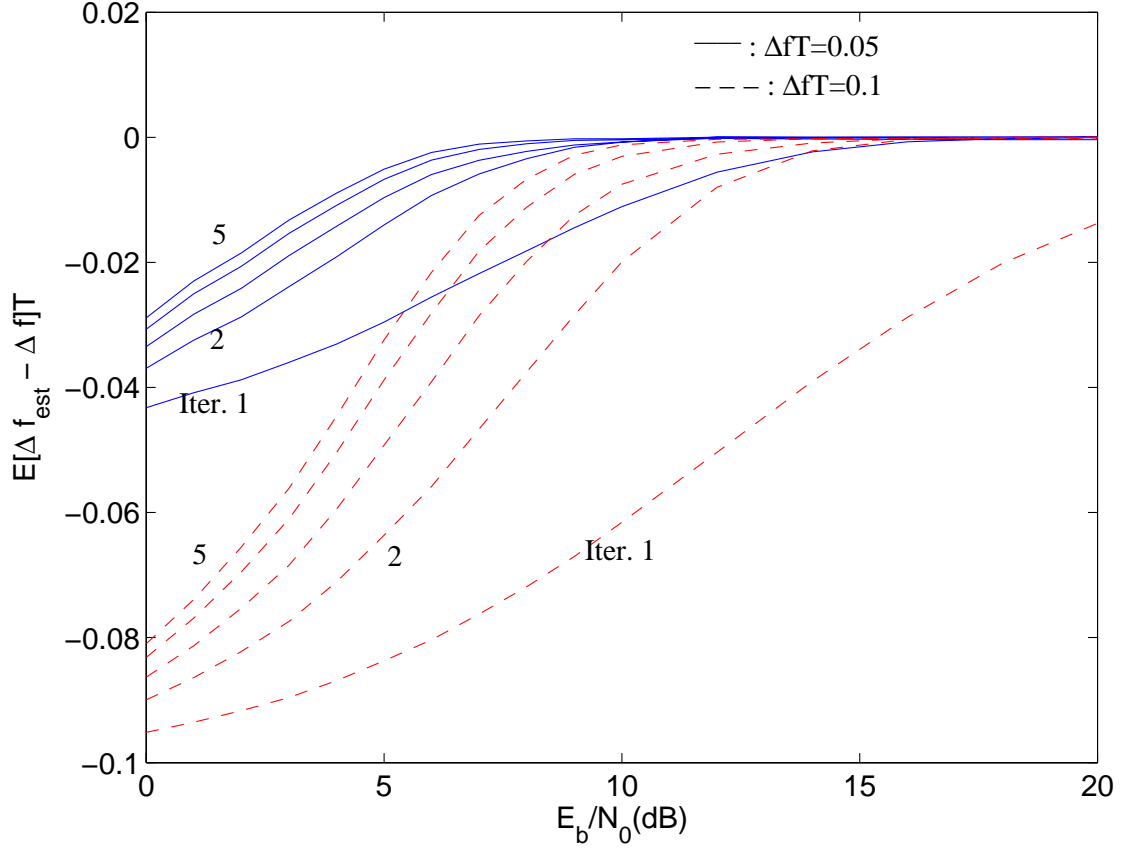


Fig. 7. Evolution of  $E[\widehat{\Delta f} - \Delta fT]$  for IFDE-SD, when  $L = 1$  and  $\Delta fT = 0.1$  or  $0.15$ .

Our results shown that the proposed receiver structures have excellent performances, allowing good BER, even with moderate frequency offsets and severely time-dispersive channels.

#### APPENDIX A

Without loss of generality, let us assume that there is no frequency error. For the sake of simplicity we will also assume that  $s_n$  is constant and real (i.e.,  $s_n = s$ ). In this case,  $y_n = s + \nu_n$  and

$$y_m y_n^* s_m^* s_n = s^4 + s^3(\nu_n^* + \nu_m) + s^2 \nu_n^* \nu_m \approx s^4 + s^3(\nu_n^* + \nu_m), \quad (32)$$

where the approximation is valid for moderate and high SNR values. If we write  $\nu_n$  (and  $\nu_m$ ) as  $\nu_n = \nu_n^I + j\nu_n^Q$ , with  $\nu_n^I = \text{Re}\{\nu_n\}$  and  $\nu_n^Q = \text{Im}\{\nu_n\}$ , then

$$y_m y_n^* s_m^* s_n \approx s^4 + s^3(\nu_n^I - j\nu_n^Q + \nu_m^I + j\nu_m^Q). \quad (33)$$

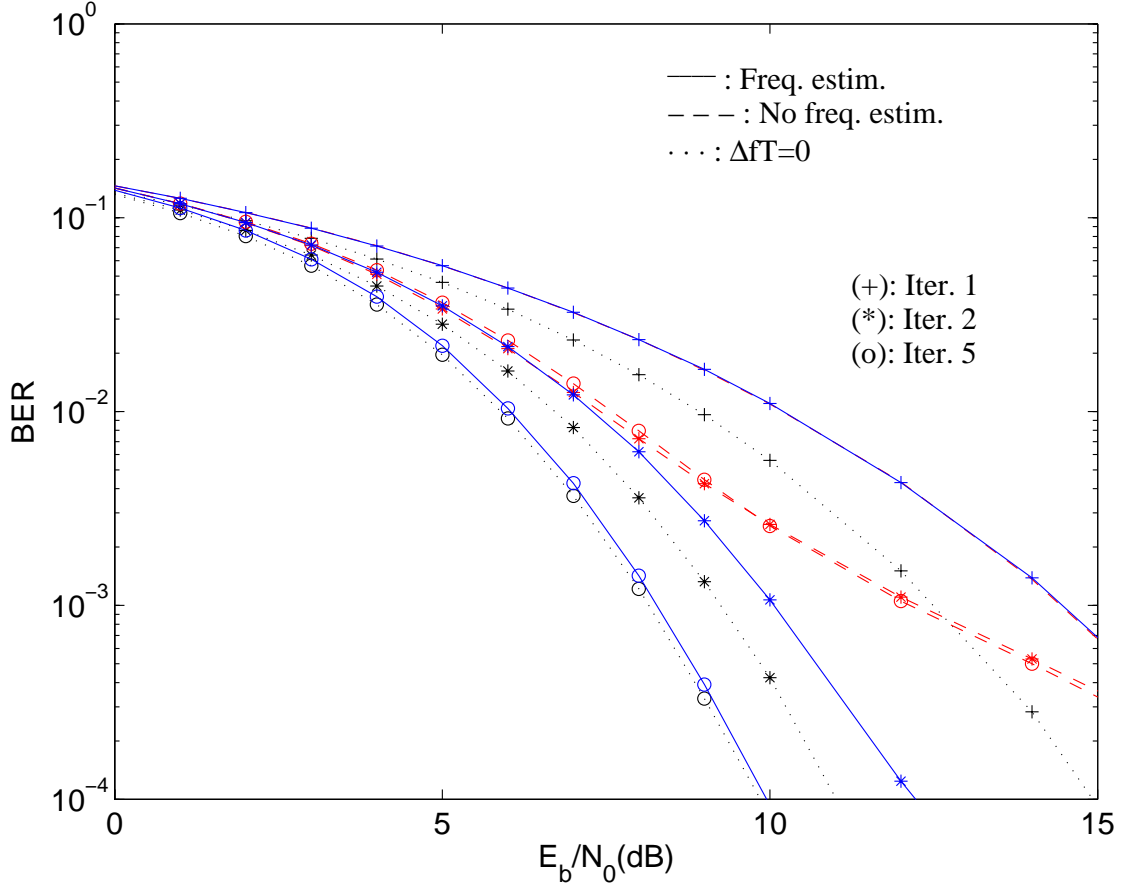


Fig. 8. Uncoded BER performance for IFDE-SD, when  $L = 1$  and  $\Delta fT = 0.05$ .

This means that the variance of the real and imaginary parts of the noise component in (33) are approximately given by  $2s^6\sigma^2$ .

If  $M > N/2$  the different noise components in the sum are uncorrelated and, since we have  $(N - M)$  terms, the variance of the real and imaginary parts of  $\xi$  is approximately given by

$$2(N - M)\sigma^2 s^6 = s^8 \frac{N - M}{SNR}, \quad (34)$$

with  $SNR = E[|s_n|^2]/E[|\nu_n|^2] = s^2/E[|\nu_n|^2]$ .

When  $M < N/2$ ,  $\xi$  can be written as

$$\xi = \sum_{n=0}^{M-1} \sum_l y_{n+M+lM} y_{n+lM}^* s^2, \quad (35)$$

where  $l$  ranges from 0 to  $\lfloor N/M \rfloor$  if  $0 \leq n \leq N \bmod M$  and from 0 to  $\lfloor N/M \rfloor - 1$  otherwise ( $\lfloor x \rfloor$  denotes 'larger integer not higher than  $x$ ' and  $x \bmod y$  denotes the 'remainder of the division between  $x$

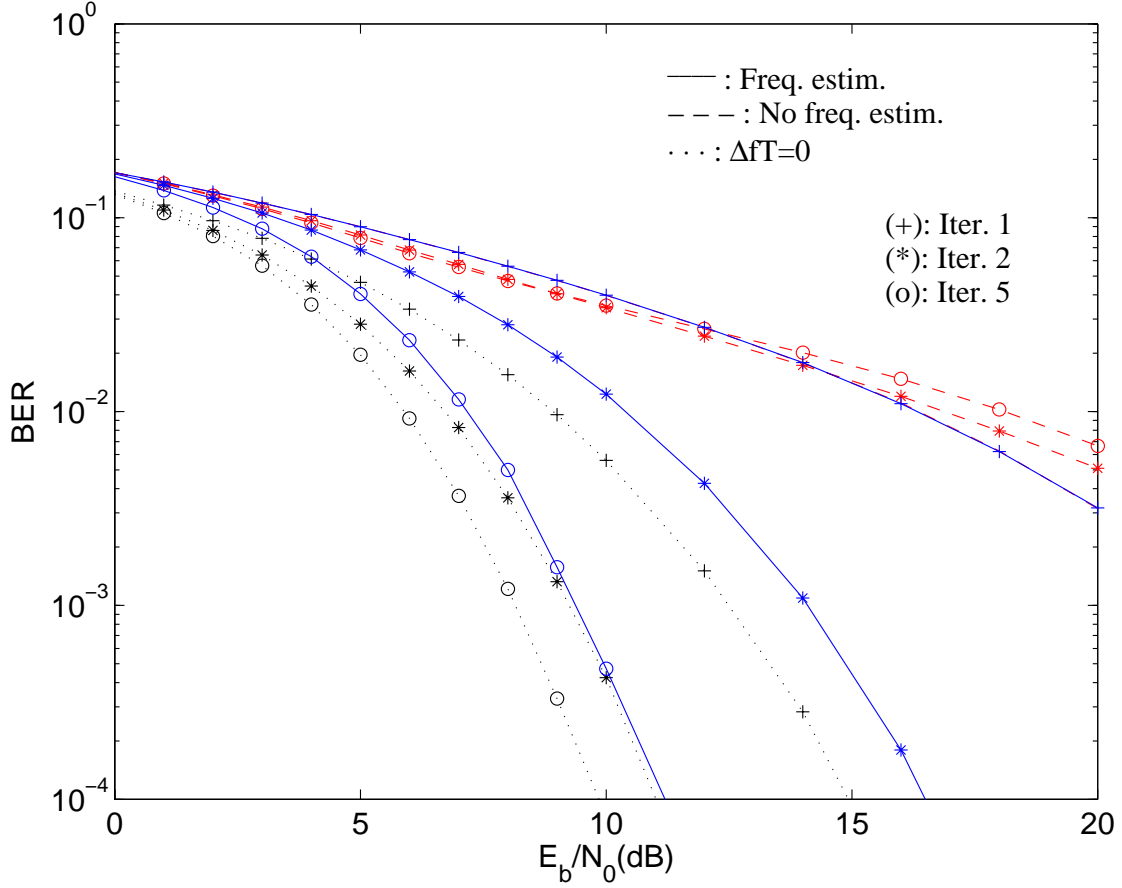


Fig. 9. Uncoded BER performance for IFDE-SD, when  $L = 1$  and  $\Delta fT = 0.1$ .

and  $y'$ ). Although the  $M$  terms associated to the first sum are uncorrelated, this is not true for the terms associated to the second sum. In fact, the noise component associated to

$$\sum_{l=0}^t y_{n+M+lM} y_{n+lM}^* \quad (36)$$

is approximately given by

$$\begin{aligned} & \sum_{l=0}^t s(\nu_{n+lM}^I - j\nu_{n+lM}^Q + \nu_{n+lM+M}^I + j\nu_{n+lM+M}^Q) = \\ & = s \left( \nu_n^I + \nu_{n+tM+M}^I + 2 \sum_{l=1}^t \nu_{n+lM}^I - j\nu_n^Q + j\nu_{n+tM+M}^Q \right). \end{aligned} \quad (37)$$

This means that the noise quadrature component of  $\xi$  has variance

$$2M\sigma^2 s^6 = s^8 \frac{M}{\text{SNR}}. \quad (38)$$

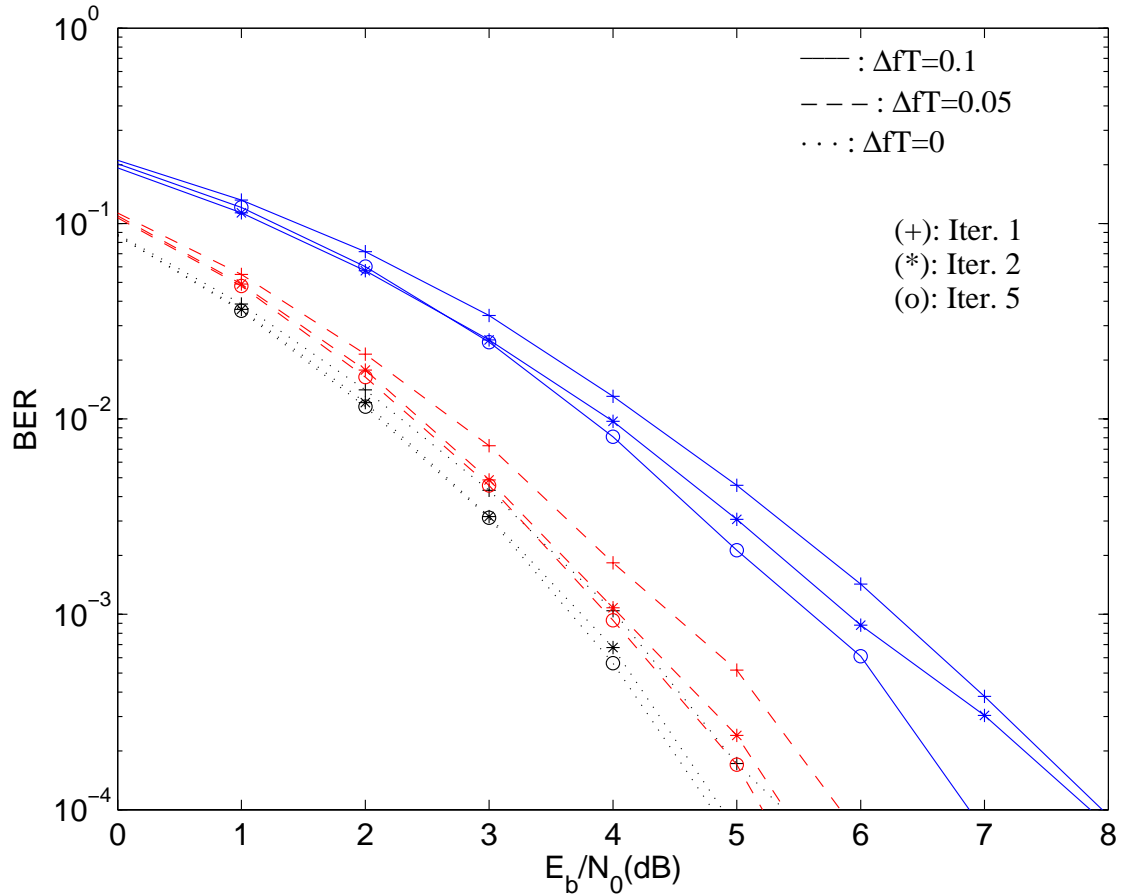


Fig. 10. Coded BER performance for IFDE-SD, when  $L = 1$  and  $\Delta fT = 0.05$  or  $0.1$ .

#### REFERENCES

- [1] L. Cimini Jr., "Analysis and Simulation of a Digital Mobile Channel using Orthogonal Frequency Division Multiplexing", *IEEE Trans. on Commun.*, Vol. 33, pp. 400-411, July 1985.
- [2] H. Sari, G. Karam and I. Jeanclaude, "An Analysis of Orthogonal Frequency-division Multiplexing for Mobile Radio Applications", *In Proc. IEEE Vehic. Tech. Conf., VTC'94*, pp. 1635-1639, Stockholm, Sweden, June 1994.
- [3] A. Gusmão, R. Dinis and N. Esteves, "On Frequency-domain Equalization and Diversity Combining for Broadband Wireless Communications", *IEEE Trans. on Commun.*, pp. 1029-1033, July 2003.
- [4] A. Gusmão, R. Dinis, J. Conceição and N. Esteves, "Comparison of Two Modulation Choices for Broadband Wireless Communications", *In Proc. IEEE Vehic. Tech. Conf., VTC'2000 (Spring)*, pp. 1300-1305, Tokyo, Japan, May 2000.

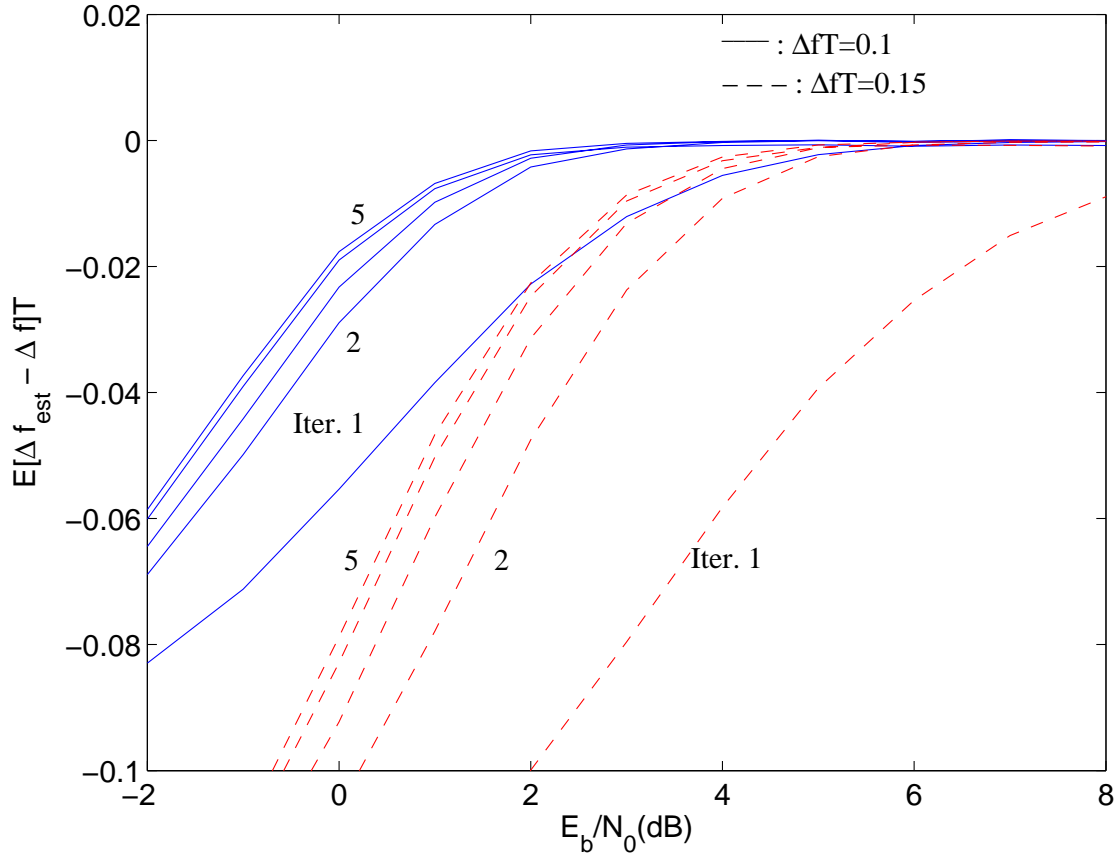


Fig. 11. Evolution of  $E[\widehat{\Delta f} - \Delta f]$  for IFDE-SD, when  $L = 1$  and  $\Delta fT = 0.1$  or  $0.15$ .

- [5] R. Dinis, A. Gusmão, and N. Esteves, "On Broadband Block Transmission over Strongly Frequency-Selective Fading Channels", in *Wireless 2003*, Calgary, Canada, July 2003.
- [6] D. Falconer, S. Ariyavisitakul, A. Benyamin-Seeyar and B. Eidson, "Frequency Domain Equalization for Single-Carrier Broadband Wireless Systems", *IEEE Commun. Mag.*, Vol. 4, No. 4, April 2002.
- [7] N. Benvenuto and S. Tomasin, "Block Iterative DFE for Single Carrier Modulation", *IEE Electronic Letters*, Vol. 39, No. 19, Sept. 2002.
- [8] R. Dinis, R. Kalbasi, D. Falconer and A. Banihashemi, "Iterative Layered Space-Time Receivers for Single-Carrier Transmission over Severe Time-Dispersive Channels", *IEEE Commun. Letters*, Vol. 8, No. 9, pp. 579–581, Sep. 2004.
- [9] M. Tüchler, R. Koetter and A. Singer, "Turbo Equalization: Principles and New Results", *IEEE Trans. on Comm.*, Vol. 50, pp. 754-767, May 2002.

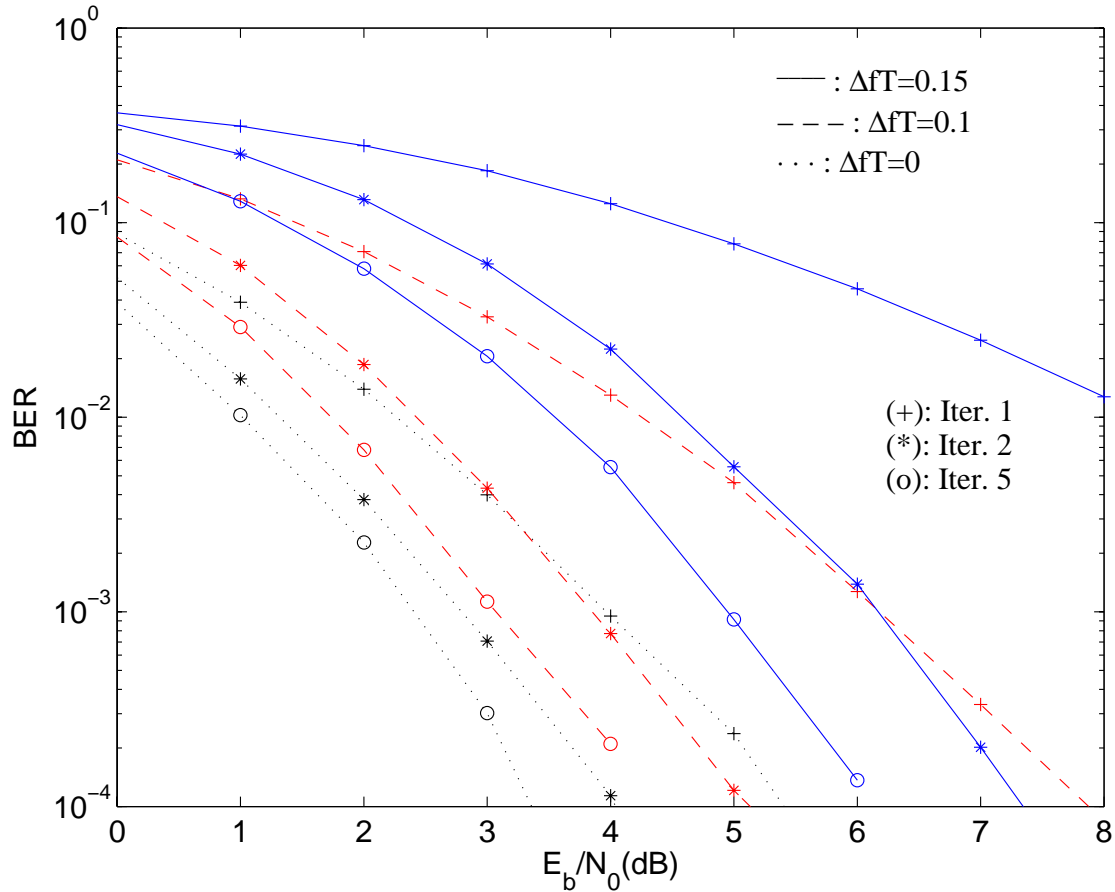


Fig. 12. Coded BER performance for the Turbo FDE, when  $L = 1$  and  $\Delta fT = 0, 0.1$  or  $0.15$ .

- [10] M. Tüchler and J. Hagenauer, "Turbo Equalization Using Frequency Domain Equalizers," *Allerton Conf.*, Oct. 2000.
- [11] M. Tüchler and J. Hagenauer, "Linear Time and Frequency Domain Turbo Equalization", *IEEE VTC'01 (Fall)*, Oct. 2001.
- [12] H. Meyr, M. Moeneclaey and S. Fetchel, *Digital Communication Receivers*, 2nd ed., Wiley Series on Telecommunications and Signal Processing, New York: Wiley, 1998.
- [13] J. Olmos, R. Agustí and F. Casadevall, "Decision Feedback Equalization and Carrier Recovery in 140Mbit QAM Digital Radio Systems", in *Proc. IEEE ICC'88*, Philadelphia, PA, 1988.
- [14] A. Czylik, "Low Overhead Pilot-aided Synchronization for Single Carrier Modulation with Frequency Domain Equalization", in *Proc. IEEE GLOBECOM'98*, pp. 2068-2073, Sydney, Australia, Nov. 1998.

- [15] P. Moose, "A Technique for Orthogonal Frequency Division Multiplexing Frequency Correction", *IEEE Trans. Commun.*, Vol. 42, pp. 2908-2914, Oct. 1994.
- [16] T. Schmidl and D. Cox, "Robust Frequency and Timing Synchronization for OFDM", *IEEE Trans. Commun.*, Vol. 45, pp. 1613-1621, Dec. 1997.
- [17] M. Morelli and U. Mengali, "An Improved Frequency Offset Estimator for OFDM Applications", *IEEE Commun. Lett.*, Vol. 3, pp. 75-77, Mar. 1999.
- [18] M. Morelli and U. Mengali, "Carrier-Frequency Estimation for Transmissions over Selective Channels", *IEEE Trans. Commun.*, Vol. 48, pp. 1580-1589, Sept. 2000.
- [19] S. Reinhardt and R. Weigel, "Pilot Aided Timing Synchronization for SC-FDE and OFDM: A Comparison", in *Proc. IEEE ISCIT'04*, Sapporo, Japan, pp. 628-633, Oct. 2004.
- [20] H. Chen and G. Pottie, "A Comparison of Frequency Offset Tracking Algorithms for OFDM", in *Proc. IEEE Globecom'03*, San Francisco, CA, pp. 1069-1073, Dec. 2003.
- [21] B. Vucetic and J. Yuan, *Turbo Codes: Principles and Applications*, Kluwer Academic Publ., Boston, 2002.
- [22] ETSI, "Channel models for HIPERLAN/2 in Different Indoor Scenarios", *ETSI EP BRAN 3ERI085B*, pp. 1-8, Mar. 1998.